THEORETICAL & APPLIED MECHANICS LETTERS **4**, 021004 (2014)

Study on the thermal protection performance of superalloy honeycomb panels in high-speed thermal shock environments

Dafang Wu,[1, a)] Anfeng Zhou,[1] Liming Zheng,[2] Bing Pan,[1] Yuewu Wang[1]
[1)]*School of Aeronautic Science and Engineering, Beijing University of Aeronautics and Astronautics, Beijing 100191, China*
[2)]*School of Astronautics, Beijing University of Aeronautics and Astronautics, Beijing 100191, China*

(Received 21 November 2013; revised 17 January 2014; accepted 29 January 2014)

Abstract The thermal protection performance of superalloy honeycomb structure in high-temperature environments are important for thermal protection design of high-speed aircrafts. By using a self-developed transient aerodynamic thermal simulation system, the thermal protection performance of superalloy honeycomb panel was tested in this paper at different transient heating rates ranging from 5°C/s to 30°C/s, with the maximum instantaneous temperature reaching 950°C. Furthermore, the thermal protection performance of superalloy honeycomb structure under simulated thermal environments was computed for different high heating rates by using 3D finite element method, and a comparison between calculational and experimental results was carried out. The results of this research provide an important reference for the design of thermal protection systems comprising superalloy honeycomb panel.

 [doi:10.1063/2.1402104]

Keywords superalloy honeycomb panel, thermal shock, high temperature, numerical simulation

With continuous improvement of the design speed of hypersonic vehicles, the problem of aerodynamic heating is becoming increasingly serious. To avoid damage to the aircraft structure and internal devices due to high temperatures resulting from severe aerodynamic heating, excellent thermal protection systems (TPSs) must be well designed for hypersonic vehicles.

Superalloy honeycomb structure is light in weight and has a strong resistance to deformation under high temperatures with lower thermal conductivity and other advantages, which makes it an ideal heat-resistant design for aerospace structures. Currently, superalloy honeycomb structures are widely used in the field of aerospace. When applied to TPS, the heat-transfer characteristics of superalloy honeycomb structures are very important for thermal protection design. Many scholars have studied this problem.[1–9] At present, it is found in most heat-transfer studies of honeycomb structure that the heat-transfer properties and effective thermal conductivity were computed using approximate numerical method or semi-empirical formulas. In contrast, few works report the finite element calculation on the thermal protection performance using a 3D model, which simultaneously considers the heat conduction in metallic materials, internal radiation, and air heat transfer within a honeycomb core, and make a comparison against the experimental results. The

[a)]Corresponding author. Email: wdf1950@163.com.

experimental studies on the thermal protection performance of superalloy honeycomb panels subjected to severe thermal shock conditions, with a high heating rate that occurs in the first stage of the launching, rising and reentry period of high-speed air vehicles, have not been reported.

In this paper, a transient aerodynamic heating simulation system was established to investigate the thermal protection performance of the superalloy honeycomb structure at different transient heating rates ranging from 5°C/s to 30°C/s, with the maximum instantaneous temperature of up to 950°C. Furthermore, the thermal protection performance of the superalloy honeycomb structure in simulated environments was determined for different high heating rates by using a 3D finite element method (FEM), and a comparison between calculational and experimental results was carried out to verify the reliability and validity of the numerical simulation and provide a basis for the thermal protection design of high-speed air vehicles.

The schematic diagram and photograph of the superalloy honeycomb structure are shown in Fig. 1. It can be seen that, the test specimen is a superalloy honeycomb panel structure consisting of front and rear high-temperature alloy plates with honeycomb core structures welded together. The square specimen has a side length of 200 mm and a total thickness of 7.82 mm, and the circumscribed circle of each honeycomb core unit has a diameter of 6 mm. The honeycomb core is 7.5 mm in height, both front and rear surface plates are 0.16 mm in thickness. In this study, the honeycomb core units were composed of trapezoidal corrugated board welded together. Each hexagon core unit has two sides with a thickness of 0.152 mm which is twice of 0.076 mm, the thickness of the other four sides of the hexagon core unit. The front and the rear panels are composed of a Ni-based high-temperature alloy GH3039. It is single-phase austenite solid solution reinforced alloy with excellent resistance to oxidation and high strength at elevated temperatures. The honeycomb core, made of GH536, is a kind of superalloy with excellent oxidation resistance in a high temperature environment of 1 200°C.

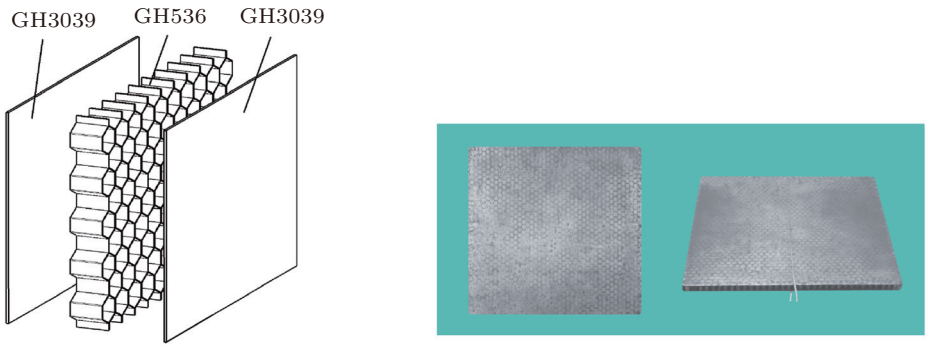

Fig. 1. Schematic diagram and photograph of the honeycomb panel structure.

The K-type thermocouples were installed on the centers of both the front and the rear surfaces to control the thermal environment and measure the thermal protection performance of the superalloy honeycomb structure at different temperatures during the experiment. By recording and analyzing the temperature difference change between the front and rear surfaces, the thermal protection performance characteristics of the superalloy honeycomb panel were obtained.

In this paper, a self-developed dynamic high-temperature environments testing system was es-

tablished and the dynamic rapid thermal shock test on the front surface of superalloy honeycomb structure was performed by this system. Figure 2 illustrates that the setup is a close looped control system and is composed of quartz infrared radiators, temperature sensors, signal amplifier, A/D converter, controlling computer, D/A converter, phase shift trigger, and high power voltage conditioner. Considering the characteristics of the simulated high-speed thermal shock environments in this test, an intelligent control strategy characterized by high adaptability to parameters changes, fast dynamic response speed and excellent robustility[10,11] was employed to realize the simulation. The thermal control system can also achieve an accurate dynamic simulation of a rapidly changing nonlinear thermal environment with a heating rate of 210°C/s, and the instantaneous test temperature of the quartz lamp infrared radiation heater can reach 1 550°C.[12]

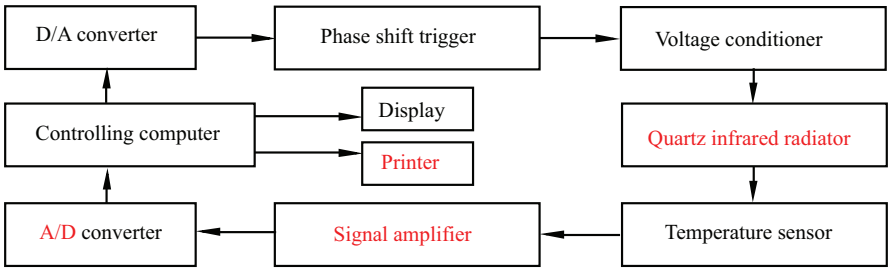

Fig. 2. Schematic diagram of the simulation system for infrared radiant aerodynamic thermal test.

Six transient thermal shock environments were established, denoted as T_1, T_2, T_3, T_4, T_5, and T_6, with heating rates of 30°C/s, 25°C/s, 20°C/s, 15°C/s, 10°C/s, and 5°C/s, respectively (Fig. 3). The front surface of the superalloy honeycomb panel was rapidly heated according to its predetermined heating rate using the experimental system. To determine the thermal protection performance of the superalloy honeycomb panel in different thermal shock environments, the temperature sensor welded on the rear surface of the panel was used to measure and record the temperature changes of the rear surface during the entire process, while the thermal shock environment of the panel's front surface was controlled.

Figure 3 shows the actual results of the controlled surface temperature of the test piece where the thermal condition with different heating rates were denoted as T_1', T_2', T_3', T_4', T_5', and T_6'. It can be seen from Fig. 3 that the controlled temperature profiles on the front surface of honeycomb structure agree well with the pre-set temperature profiles throughout the entire experiment.

Due to length limitations of this paper, only the pre-set temperature values and the actual control results for the heating rate of 30°C/s at 5 s, 10 s, ..., 30 s are provided in Table 1. As shown in the table, the relative errors between the actual and the pre-set temperature of all points were less than 1.0%. This result proves that the experimental simulation can achieve a high accuracy for tracking the control of transient thermal shock environments.

The test result curves on the rear surface of the honeycomb structure are illustrated in Fig. 4 when the front surface temperature curve was T_1 (30°C/s). It can be seen that, for the superalloy honeycomb structure test specimen, when the front surface was heated by a thermal shock with a constant temperature rising rate, the rear surface temperature, denoted as T_{1b} in Fig. 4, increased nonlinearly. Based on the rapid dynamic changes of the front and rear surface temperatures,

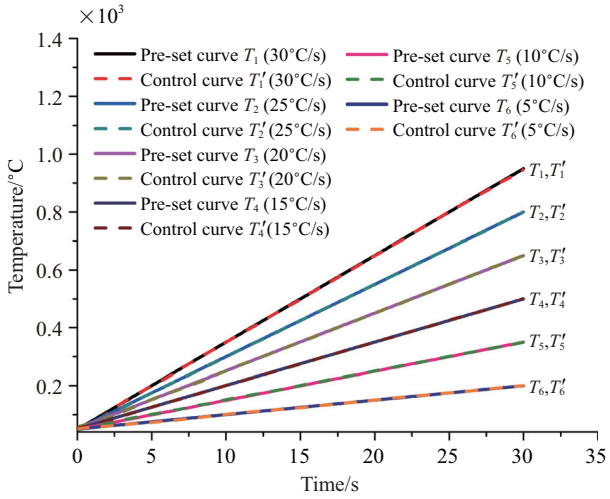

Fig. 3. Pre-set and controlled temperature curves on the front surface of the superalloy honeycomb panel.

Table 1. Pre-set and controlled temperature on the front surface of the superalloy honeycomb panel at heating rate of 30°C/s.

Time/s	5	10	15	20	25	30
Pre-temperature/°C	200	350	500	650	800	950
Control temperature/°C	198.5	349.7	498.7	649.5	801.4	947.5
Relative error/%	−0.75	−0.09	−0.26	−0.08	0.17	−0.26

the thermal protection performance of the superalloy honeycomb structure was obtained at each moment for different heating rates.

Figure 5 illustrates the temperature differences for the front and the rear surfaces of the superalloy honeycomb structure heated under six different heating rates. It shows that the temperature differences between the front and rear surfaces changed quite rapidly during the first ten seconds, then varied mildly gradually, and tended to stationary after 20 s. Moreover, the temperature difference of the superalloy honeycomb structure reached 372°C when the front surface reached 950°C, indicating that the superalloy honeycomb panel provides, to certain extent, an effective thermal protection. The temperature differences at different heating rates obtained in this work offer an important basis for the thermal protection design of superalloy honeycomb panels in thermal shock environments.

Images of the deformed superalloy panel (200 mm×200 mm×1.56 mm) and the deformed superalloy honeycomb panel (200 mm×200 mm×7.82 mm) after the high-temperature experiments up to 950°C are shown in Fig. 6. The superalloy panel (Fig. 6(a)) becomes severely bent and twisted after being exposed to a 950°C high-temperature environment. However, the flexure and deformation of the superalloy honeycomb panel (Fig. 6(b)) was very slight after the 950°C high-temperature thermal environment experiment. This test demonstrates that the superalloy honeycomb panel was suitable as a structural component that requires light-weight and low-deflection

 doi:10.1063/2.1402104

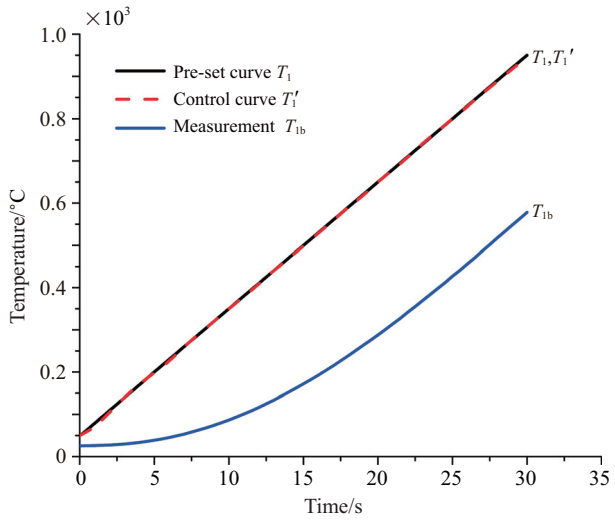

Fig. 4. Temperature on the rear surface of superalloy honeycomb panel at heating rate of 30°C/s.

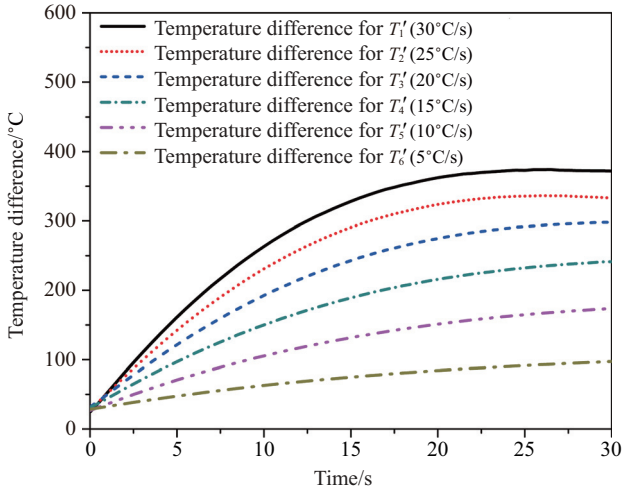

Fig. 5. Temperature difference between the front and rear surfaces of honeycomb panel at different heating rates.

properties on high-speed aircrafts which experience high-temperature aerodynamic heating.

The inner heat transfer of the superalloy honeycomb structure is very complicated and includes heat conduction in metal materials, heat radiation among the metal inner wall surfaces and air heat convection in honeycomb cavity. The heat exchange between the rear surface of test specimen and the surroundings includes air natural convection and radiation heat dissipation to the surroundings. These three kinds of heat transfer, e.g., heat conduction, heat convection, and radiation, should all be considered in the numerical simulation.

The planar dimensions of the superalloy honeycomb panel are 200 mm×200 mm, and its total thickness is only 7.82 mm. The width to thickness ratio is 25.6. Therefore, the adiabatic boundary on the four sides has little effect on the central region of the superalloy honeycomb

(a) high-temperature alloy panel (b) superalloy honeycomb panel

Fig. 6. Distortion of high-temperature alloy panel and superalloy honeycomb panel after 950°C heating.

panel. As a result, one honeycomb unit was extracted from the honeycomb structure, as shown in Fig. 7(a), to create a finite element model in the numerical simulation. The finite element model is depicted in Fig. 7(b), and the figure shows that the wall thicknesses of the two welding sides are 0.076 mm (2δ) and the thickness of the other four sides are 0.038 mm (δ). The finite element mesh is shown in Fig. 7(c), a hexahedral 8-node finite element was adopted in the numerical simulation, and the honeycomb unit solid model was divided into 13 286 finite element units with 17 617 nodes in this numerical simulation.

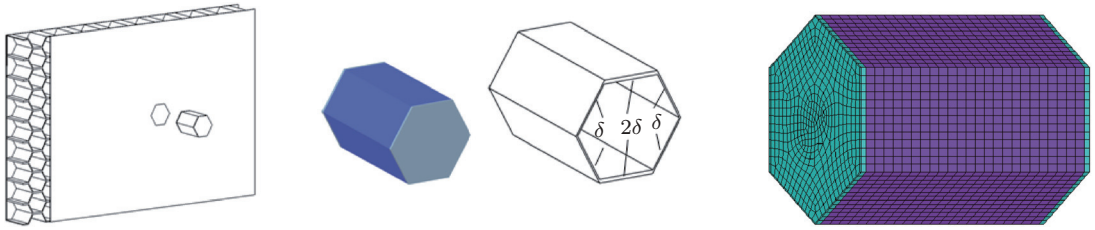

(a) (b) (c)

Fig. 7. Honeycomb unit model and finite element grid.

In the numerical simulation, the temperature on the front surface of the honeycomb model was known and preset by the thermal test simulation in accordance with the predetermined temperature curves, therefore, it is a boundary condition of the first kind applied on the front surface of the superalloy honeycomb structure. Six temperature changes at various heating rates are shown as curves T_1–T_6 in Fig. 3.

The heat exchange between rear surface and surroundings includes the natural convection and radiation heat transfer. For the calculation of the heat flux in natural convection heat transfer as well as the involved physical parameters of air, please refer to Ref. 13. The emissivity of the internal wall surface of the enclosed honeycomb units and the rear surface involved the radiation heat transfer are chosen to be 0.8.[13] The thermal conductivity and the specific heat capacity of GH3039 and GH536 alloys at different temperatures can be found in Ref. 14.

The calculated results of heat transfer process for the honeycomb structure at 30 s are given in this paper. Figure 8 illustrates the temperature distribution of the superalloy honeycomb unit under T_1, including the temperature distributions at $t = 15$ s and $t = 30$ s. The reason for the selection of a time of $t = 15$ s was that it was the half-way point of the overall 30 s experiment, and the $t = 30$ s point was chosen because this was the moment when the temperature of the front surface reached its maximum value.

The test and numerical simulation results curves on the rear surface corresponding to T_1, T_2,

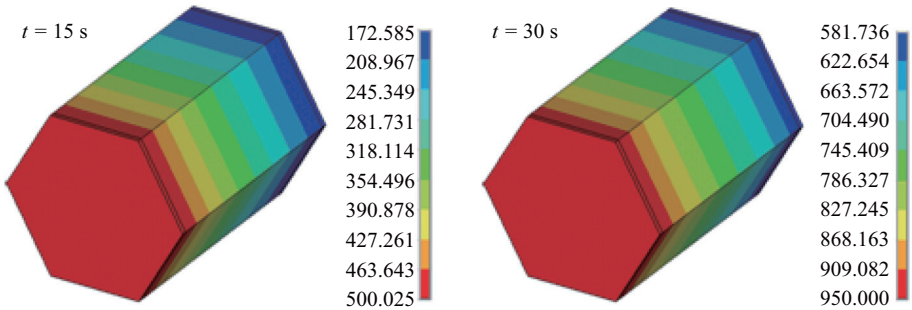

Fig. 8. The superalloy honeycomb panel unit temperature field at heating rate of 30°C/s.

T_3, T_4, T_5, and T_6 are presented in Fig. 9. It can be seen from Fig. 9 that, the calculated results by the numerical method agreed well with the measured curves of temperature variation by the thermocouples on the rear surface of the specimen during the experiment.

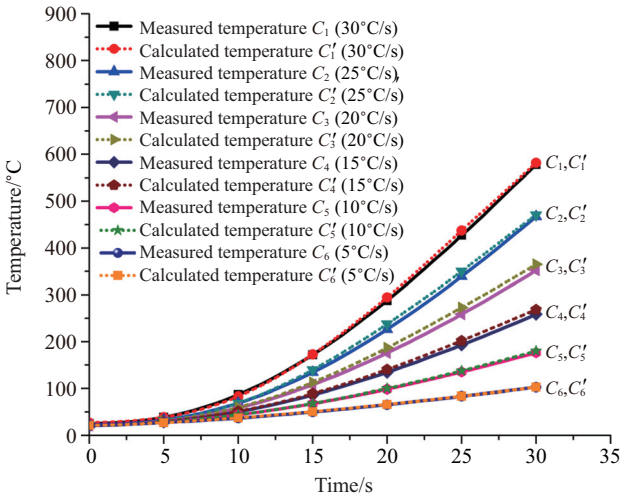

Fig. 9. Calculated and experimental results on the rear surface at different heating rates.

Moreover, partial data of the measured and calculated results on the rear surface of the specimen under six different heating rates are collected in Table 2. The slight relative difference $(C_1'–C_1)/C_1$ between the calculated and measured results illustrated in Table 2 verifies the validity of the present numerical simulation.

Using the self-developed dynamic high-temperature environments testing system, the dynamic rapid thermal shock test on the front surface of superalloy honeycomb structure was also performed. The thermal protection performance of the superalloy honeycomb structure was experimentally investigated in transient thermal shock environments, and the heat insulation effects of the panel at various heating rates were obtained (the maximum heating rate was 30°C/s and the ultimate instantaneous temperature was 950°C).

The thermal protection performance of the superalloy honeycomb structure in simulated environments was determined for different high heating rates by using the 3D finite element method.

Table 2. Measured and calculated results on rear surface of superalloy honeycomb panel at heating rate of 30°C/s.

Time/s	5	10	15	20	25	30
Measurement C_1/°C	38.8	86.7	171.9	287.7	427.2	578.1
FEM C_1'/°C	38.7	83.4	172.6	294.5	437.3	581.7
$(C_1'-C_1)C_1^{-1}$/%	−0.26	−3.81	0.41	2.36	2.36	0.62

The fact that the calculation results agrees well with the test results demonstrates the reliability and validity of the numerical method and the test method. The good agreements also confirm the feasibility to replace costly aerodynamic heating tests by numerical simulations.

The experiment reveals that after being subjected to a high-temperature load of 950°C, the superalloy honeycomb panel still has a strong deformation-resistant capability, with its light-weight characteristics as well as thermal protection performances. Thus the superalloy honeycomb panel structure may have an important engineering application significance and a prospect of wide application in the thermal protection design of high-speed aircrafts.

This work was supported by the National Natural Science Foundation of China (11172026 and 91216301) and the Specialized Research Fund for the Doctoral Program of Higher Education (20131102110014).

1. R. T. Swann, C. M. Pittman. Analysis of effective thermal conductivities of honeycomb-core corrugated-core sandwich panels. NASA Technical Note D-714 (1961).
2. D. K. Edwards, J. N. Arnold, P. S. Wu. Correlations for natural convection through high L/D rectangular cell. *Journal of Heat Transfer* **101**, 741–743 (1979).
3. T. Fusegi, J. M. Hyun, K Kuwahara, et al. A numerical study of three dimensional natural convection in a differentially heated cubical enclosure. *International Journal of Heat and Mass Transfer* **34**, 1543–1557 (1991).
4. Y. Asako, Y. Yamaguchi, L. Chen, et al. Combined natural convection and radiation heat transfer in a vertical air cavity with hexagonal honeycomb core of negligible thickness. *Numerical Heat Transfer, Part A* **30**, 73–85 (1996).
5. D. W. Pepper, K. G. T. Hollands. Summary of benchmark numerical studies 3-D natural convection in an air-filled enclosure. *Numerical Heat Transfer, Part A* **42**, 1–11 (2002).
6. T. Wen, J. Tian, T. J. Lu, et al. Forced convection in metallic honeycomb structures. *International Journal of Heat and Mass Transfer* **49**, 3313–3324 (2006).
7. S. T. Liu, Y. C. Zhang, P. Liu. New analytical model for heat transfer efficiency of metallic honeycomb structures. *International Journal of Heat and Mass Transfer* **51**, 6254–6258 (2008).
8. Y. Y. Tang, M. D. Xue. Thermo-mechanical characteristics analysis of sandwich panel with honeycomb core. *Acta Materiae Compositae Sinica* **22**, 130–136 (2005) (in Chinese).
9. L. Jing, G. F. Wang, S. F. Tang, et al. Radiation and conduction coupling problems of honeycomb sandwich panel. *Journal of Harbin Institute of Technology* **42**, 827–831 (2010) (in Chinese).
10. D. F. Wu, Y. W. Wang, S. Wu, et al. Research on control of heat flux environment simulation for high-speed aircraft *Advanced Materials Research* **705**, 528–533 (2013)
11. D. F. Wu, S. Wu, Y. W. Wang, et al. Rapid high-precision non-linear calibration for temperature sensors in transient aerodynamic heating simulation systems. *Applied Mechanics and Materials* **321–324**, 618–623 (2013).
12. D. F. Wu, B. Pan, Z. T. Gao, et al. On the experimental simulation of ultra-high temperature, high heat flux and nonlinear aerodynamic heating environment and thermo-machanical testing technique. *Journal of Experimental Mechanics*, **27**, 255–271 (2012) (in Chinese).
13. S. M. Yang, W. Q. Tao, Heat Transfer, 3rd edn. Higher Education Press, Beijing (2002) (in Chinese).
14. X. L. Song, J. R. An, New Chinese and Foreign Metallic Material Handbook, Chemical Industry Press, Beijing (2008) (in Chinese).